Contribution of Fetal MR Imaging in the Evaluation of Cerebral Ischemic Lesions

Catherine Garel, Anne-Lise Delezoide, Monique Elmaleh-Berges, Françoise Menez, Catherine Fallet-Bianco, Edith Vuillard, Dominique Luton, Jean-François Oury and Guy Sebag

AJNR Am J Neuroradiol 2004, 25 (9) 1563-1568
http://www.ajnr.org/content/25/9/1563

Contribution of Fetal MR Imaging in the Evaluation of Cerebral Ischemic Lesions

Catherine Garel, Anne-Lise Delezoide, Monique Elmaleh-Berges, Françoise Menez, Catherine Fallet-Bianco, Edith Vuillard, Dominique Luton, Jean-François Oury, and Guy Sebag

BACKGROUND AND PURPOSE: **Little is known about the different patterns of fetal cerebral ischemic lesions at MR imaging. Our purpose was to evaluate the contribution of MR imaging in the evaluation of such lesions by correlating the results with ultrasonography (US) and neurofetopathologic (NFP) findings.**

METHODS: **We examined 28 fetuses (mean, 28 weeks' gestation) with cerebral ischemic lesions on NFP examination. MR findings were correlated with US and NFP results with regard to the depiction of gyration and parenchymal abnormalities.**

RESULTS: **MR imaging added to US findings in 24 cases by revealing lesions (gyration abnormalities, parenchymal lesions). These results were either overlooked during US ($n = 16$) or more extensive than expected with US ($n = 8$). MR findings were always confirmed by NFP. NFP yielded additional findings for 14 lesions that were overlooked during MR imaging ($n = 4$) or that were more extensive than expected with MR imaging ($n = 10$). T1-, T2-, and T2*-weighted MR patterns of different lesions (cavitations, gliosis, softening of the white matter, laminar necrosis, calcified leukomalacia, old hemorrhage) were identified.**

CONCLUSION: **MR imaging is a valuable tool in the evaluation of fetal brain ischemia. The results of this study emphasize the role of the different sequences (T1-, T2-, T2*-weighted) required to detect fetal cerebral ischemic lesions. MR imaging is more accurate in the detection of small focal lesions than in the evaluation of diffuse white matter abnormalities.**

Some risky situations may lead to an impairment of fetal brain perfusion and subsequent cerebral ischemic lesions. Severe or prolonged hypoxia can induce fetal death or definitive cerebral lesions. The severity, type, and distribution of such lesions depend on numerous factors, which include the duration of the causal mechanism and the fetus' gestational age (1). The susceptibility of some areas to hypoxia varies with the stage of pregnancy (2).

Ischemic and hemorrhagic phenomena are often mixed because capillaries can be ruptured during reperfusion of an ischemic lesion, triggering a hemorrhage (3, 4). However, these two types of lesions may also be clearly distinguished; pure intraparenchymal ischemia is more frequent in fetal life than in the perinatal period (5).

The usefulness of fetal MR imaging in the evaluation of ischemic brain damage has been studied in a series of seven fetuses (6). The purpose of our study was to evaluate 28 fetuses presenting with ischemic cerebral lesions and to correlate the MR imaging results with ultasonography (US) and neurofetopathologic (NFP) findings.

Methods

All fetuses in whom fetal MR was performed and who presented with cerebral ischemic lesions on NFP study were included. Fetuses with extensive parenchymal hemorrhage on NFP examination were excluded so that pure ischemic parenchymal lesions could be studied. Fetuses with MR lesions highly suggestive of ischemic damage but without autopsy results were also excluded. Hence, two fetuses were excluded because of lack of NFP examination and despite diffuse ischemic lesions on MR images. One of these fetuses had a vein of Galen aneurysmal malformation, and the other was examined after the death of its monochorionic co-twin a few weeks earlier. Therefore, between 1993 and 2003, 28 fetuses were included in this study.

The causes of impaired fetal brain perfusion were investigated in every case. The gestational age at the first pathologic US examination was recorded. Sonograms obtained just before MR imaging were analyzed with regard to ventricular dilatation

Received October 7, 2003; accepted after revision February 4, 2004.

From the Departments of Pediatric Imaging (C.G., M.E.-B., G.S.), Developmental Biology (A.-L.D., F.M.), and Obstetrics and Gynecology (E.V., D.L., J.-F.O.), Hôpital Robert Debré, and the Department of Pathology (C.F.-B.), Hôpital Sainte-Anne, Paris, France.

Address reprint requests to Catherine Garel, Department of Pediatric Imaging, Hôpital Robert Debré, 48 Boulevard Sérurier, 75019 Paris, France.

TABLE 1: Etiologies of circulatory impairment in 11 fetuses

Etiology	No. of Fetuses
Vascular: preeclampsia, intrauterine growth restriction with abnormalities on uterine/cerebral Doppler study	5
Infection: toxoplasmosis, cytomegaloviral infection	3
Metabolic: diabetes with severe maternal ketoacidosis	1
Space-occupying intracranial lesion: brain tumor, huge bilateral subdural hematoma	2

TABLE 2: Classification of parenchymal lesions

No. of Lesions	Definition and Extent	
	Diffuse	Focal
Unique (n = 13)	11	2
Multiple (n = 13)	3	10

TABLE 3: MR signal-intensity patterns of the ischemic lesions

Sequence	Hypointensity	Hyperintensity
T1 weighted	17	8
T2 weighted	5	16
T2* weighted	2	0

and the depiction of gyration and parenchymal abnormalities. The mean time between MR imaging and the last pathologic US examination was recorded. MR imaging was performed by using a 0.5-T unit (Elscint; Gyrex, Haifa, Israel) (n = 14) between 1993 and 1999 or with a 1.5-T unit (Intera; Philips, Best, the Netherlands) (n = 14) between 1999 and 2003.

Maternal sedation was achieved with the oral administration of flunitrazepam (1 mg) 20–30 minutes before the examination. T1- and T2-weighted sequences were performed in all fetuses. With the 0.5-T unit, we performed a gradient-echo (GRE) T1-weighted sequence (TR/TE/NEX, 300/15/4; flip angle, 90°; matrix, 200 × 200; field of view, 320 × 320; section thickness, 5 mm) and E short-type T2-weighted, stimulated-echo, single-shot, GRE spin-echo (SE) sequence (20/9.2/12; flip angle, 70°; matrix, 200 × 200; field of view, 320 × 320; section thickness, 5 mm). With the 1.5-T unit, we performed T1-weighted SE, spectral presaturation inversion recovery (SPIR), fat-saturated sequences (697/14/2; flip angle, 90°; matrix, 256 × 256; field of view, 320 cm; rectangular field of view, 75%; section thickness, 4 mm; acquisition time, 2 minutes 56 seconds; 15 sections). T2-weighted single-shot turbo SE imaging (24,617/100/1; flip angle, 90°; turbo SE factor, 84; matrix, 256 × 256; field of view, 280 cm; rectangular field of view, 85%; section thickness, 3 mm; acquisition time, 24 seconds; 25 sections) was also performed. GRE T2*-weighted imaging was also performed in seven fetuses.

T2-weighted images were acquired in the three planes of space, and T1-weighted images were acquired in an axial or coronal plane or both. All sections were parallel or orthogonal to the brain stem.

Gyration was evaluated according to the normal data already published (7). It was considered abnormal if it was markedly delayed (more than 3 weeks) or gyration or migration abnormalities were present. The lesions observed on MR images and suggestive of an ischemic nature were described as unique or multiple and diffuse or focal, as follows: Unique was one lesion; multiple, two or more lesions; focal, well defined and localized; and diffuse, ill defined and extensive. For each examination, MR findings were correlated with US results.

The mean time between NFP examination and MR imaging was recorded. Parenchymal lesions observed with NFP were analyzed.

Results

A cause for impaired fetal brain perfusion was found in 11 fetuses (Table 1). In the remaining 17 fetuses, no cause was found.

The first pathologic US examination was performed at a mean gestational age of 28.8 ± 5 weeks (range, 21–38 weeks). Intrauterine growth restriction was observed in seven of 28 cases. Sixteen fetuses presented with ventricular dilatation, and 11 fetuses had abnormal echogenicity of the brain parenchyma suggestive of an ischemic lesion. Three fetuses presented with limited intraventricular hemorrhage. For the others, US results did not suggest hemorrhage, and only small hemorrhagic foci were observed on NFP examination in three fetuses.

MR imaging was performed at a mean gestational age of 31.8 ± 3.3 weeks (range, 23–39 weeks). The mean time between MR imaging and last pathologic US was 1.1 ± 0.75 weeks. Gyration was normal (n = 16), abnormal (n = 6), or not interpretable (n = 6) because of an excessively thin pericerebral space or poor image quality. Parenchymal lesions were classified as unique or multiple and diffuse or focal (Table 2). Signal intensity was correlated with the mirror contralateral anatomic region when lesions were focal (unique or multiple) or diffuse but unique. When lesions were diffuse and bilateral, signal intensity was correlated with the normal parenchymal appearance according to gestational age (8, 9). In two fetuses with marked ventriculomegaly, MR images did not show any parenchymal lesions. Signal intensity abnormalities were distributed as shown in Table 3.

In four cases, MR imaging confirmed the US findings. In 24 cases, MR imaging provided additional findings: In one case, MR images showed parenchymal lesions, whereas US had shown only biometrical abnormalities. In five cases, MR results were pathologic, and the study was performed because of a risk situation despite normal US results. In nine cases, MR imaging showed ischemic lesions, whereas US had depicted only ventriculomegaly. In two cases (one polymicrogyria and one subependymal heterotopia), MR images depicted gyration and/or migration abnormalities (Fig 1). MR examination also showed that the lesions were more extensive than shown by US (n = 8, including one fetus with gyration abnormalities).

The mean time between MR and NFP examination was 1.3 ± 0.95 weeks. Various types of ischemic lesions were observed during NFP: diffuse gliosis, softening of the white matter, necrosis, small cavitations, porencephaly, subependymal pseudocysts, periventricular leukomalacia with or without microcalcifications, laminar necrosis, and polymicrogyria. Small hemorrhagic foci were also found. NFP always confirmed the MR findings. In 13 fetuses, it also provided additional findings, as follows: In 10 cases,

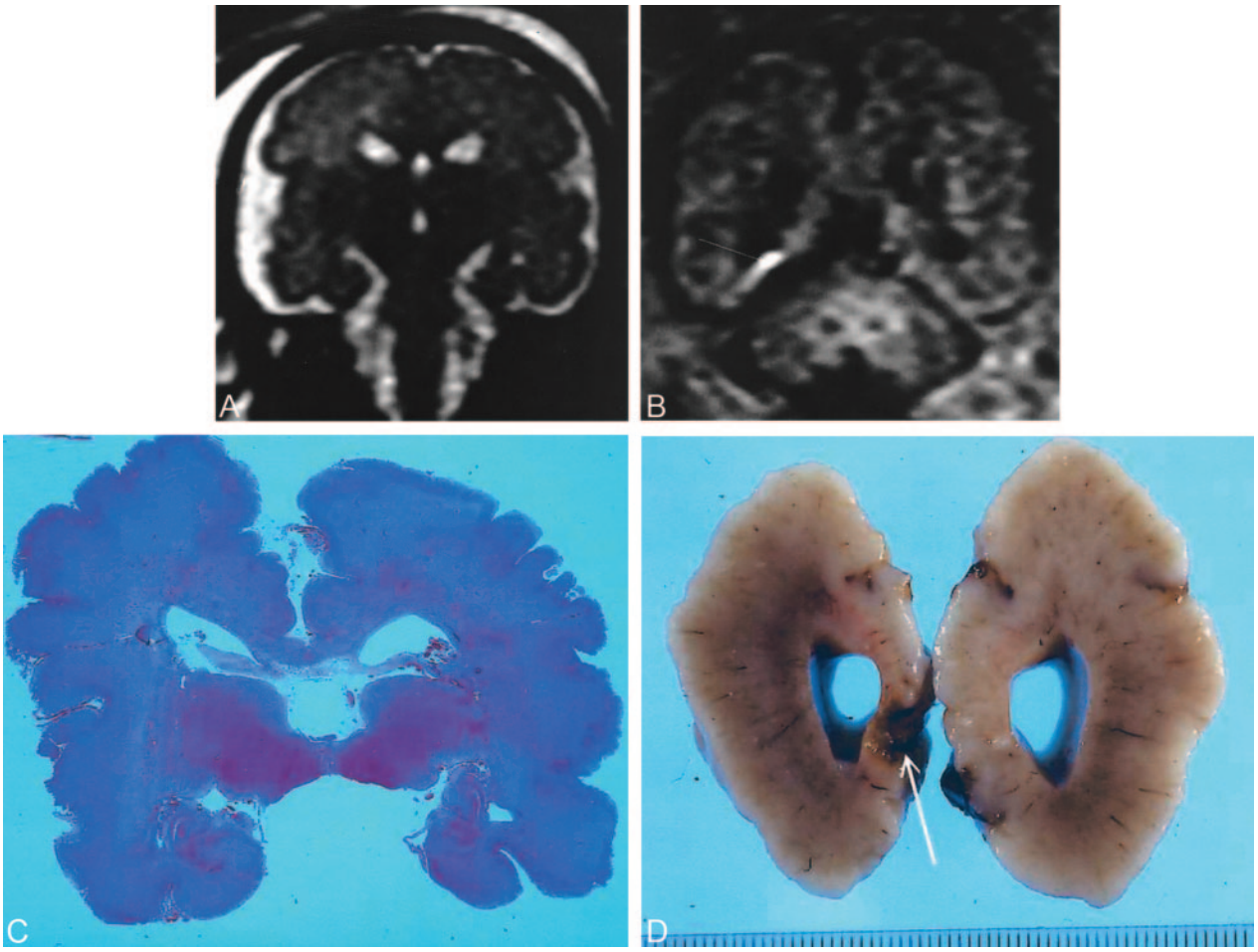

FIG 1. Transitory ventriculomegaly at 21 weeks' gestation. At 29 weeks, US revealed linear hyperechogenicities around the frontal horns. MR imaging was performed at 30 weeks.

A, T2-weighted coronal section at the level of the temporal lobes shows bilateral opercular dysplasia, gyration delay (no frontal or temporal sulci), and a polymicrogyric cortical pattern.

B, T1-weighted coronal section at the level of the atria. Hyperintensity along the inferior aspect of the right atrium (*arrow*) was overlooked on T2-weighted images. The pregnancy was terminated at 30 weeks' gestation. NFP findings confirmed gyration and parenchymal lesions.

C, Coronal histologic section at the level of the temporal lobes show diffuse polymicrogyria with opercular dysplasia.

D, Macroscopic coronal view shows right occipital cavitation (*arrow*). Calcifications were present on histologic examination.

the damage was more extensive on NFP studies than on MR imaging studies. In two cases, polymicrogyria was not expected on the basis of MR imaging findings, and one of the fetuses with polymicrogyria had more extensive damage on NFP study than expected on the basis of MR imaging findings. In two fetuses,

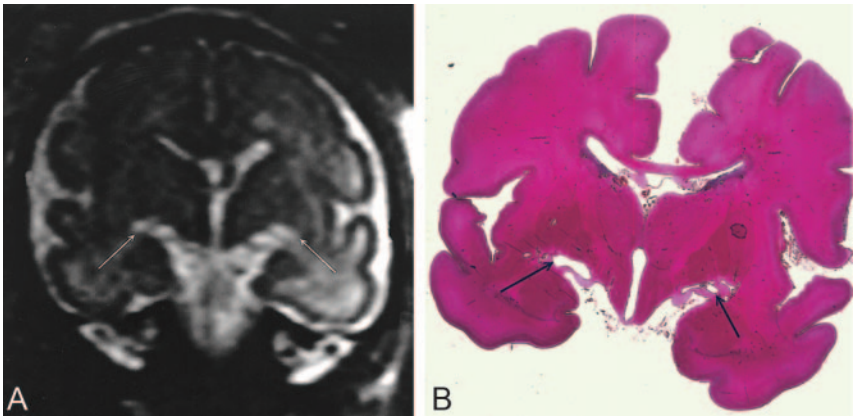

FIG 2. At 32 weeks' gestation, US showed decreased cerebellar transverse diameter (<10th percentile) without supratentorial abnormality. MR imaging was performed at 32.5 weeks. Infratentorial biometry was evaluated with MR study at about 28 weeks.

A, T2-weighted coronal section at the level of the thalami shows marked bilateral hyperintensity beneath the thalami just above the hippocampal fissure (*arrows*). Because of biometric and signal intensity abnormalities, termination of pregnancy was proposed and performed at 34 weeks. NFP confirmed the biometric abnormalities and showed a diffuse gliosis with neuronal necrosis lesions involving the cerebral peduncles, thalami, and hippocampal cortex.

B, Coronal histologic section shows bilateral cavitation (*arrows*) above both hippocampal fissures.

FIG 3. MR imaging performed at 34 weeks' gestation because of mild (12-mm) dilatation of the left lateral ventricle at US. T2-weighted axial section at the level of the vertex shows diffuse bilateral frontal hyperintensity (hypointensity on T1-weighted imaging, not shown). Images also showed left lateral ventriculomegaly (12.5 mm) and a left subependymal pseudocyst. An ischemic process was suggested and because of the diffuse frontal abnormality, a termination of pregnancy was performed at 36 weeks' gestation. NFP revealed a diffuse softening of the white matter with periventricular gliosis.

ischemic lesions were overlooked on MR images. In these two cases, termination of pregnancy was proposed because of marked (17- and 18-mm) bilateral ventriculomegaly and because of the rapid progression of unilateral ventriculomegaly (from 10 to 15 mm in 6 weeks) despite the absence of signal intensity abnormalities on MR images. NFP showed diffuse gliosis in both fetuses.

The correlation between MR and NFP findings showed the following: Focal unique or multiple T1 hypointensities and T2 hyperintensities corresponded to necrosis and cavitations (Fig 2). Diffuse T1 hypointensities and T2 hyperintensities corresponded to gliosis and/or softening of the white matter (Fig 3). Images in the case shown in Figure 3 also demonstrated left lateral ventriculomegaly (12.5 mm) and a left subependymal pseudocyst. An ischemic process was suggested and because of the diffuse frontal abnormality, a termination of pregnancy was performed at 36 weeks' gestation. NFP revealed a diffuse softening of the white matter with periventricular gliosis. Focal unique or multiple T1 hyperintensities and T2 isointensities corresponded to microcalcifications in laminar necrosis (Fig 4) or calcified leukomalacia (cf Fig 1 supra). Marked T2* hypointensity, slight T2 hypointensity, and T1 isointensity corresponded to old hemorrhage (Fig 4).

Discussion

The causes of ischemia found in 11 fetuses corresponded to what has been reported in the literature. Schematically, these causes can be of placental, fetal (infection, anasarca), or maternal (hypovolemic shock, hypoxia, abdominal trauma, hypotension or hypertension, drug use) origin (10, 11).

Atrophy of the adjacent structures due to compression may explain the ischemic lesions observed in the two fetuses with brain tumors and huge bilateral subdural hematomas. However, in the remaining 17 fe-

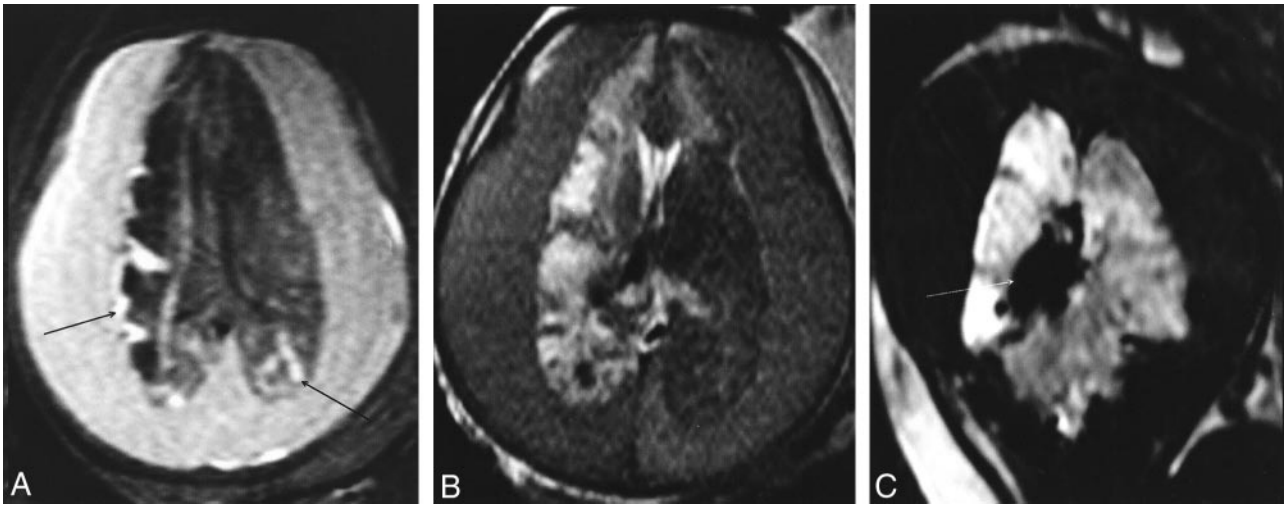

FIG 4. Huge subdural hematoma (after a fall down stairs a week earlier) in a fetus of 34 weeks' gestation. US showed the bilateral hematoma with a fluid-fluid level, an enlarged right choroid plexus, and a hyperechogenicity in the posterior part of the right hemisphere.

A and *B*, Axial T1-weighted (*A*) and T2-weighted (*B*) sections at the level of the lateral ventricles. The hematoma is hyperintense in *A* and has intermediate signal intensity in *B*. Right hemisphere and frontal part of the left hemisphere are hypointense in *A* and hyperintense in *B* in relation to gliosis. Cortical hyperintensity in the right hemisphere (*arrows*) and posterior part of the left hemisphere corresponded to laminar necrosis during NFP study (not shown).

C, T2*-weighted coronal section shows marked hypointensity of the right choroid plexus (*arrow*) in relation to hemorrhage.

tuses, no cause was found despite intensive questioning of the mother.

In this series, analysis of the correlations between US and MR findings showed that MR is more efficient than US concerning the evaluation of gyration and cerebral parenchyma.

Gyration

Two gyration and migration abnormalities were observed with MR imaging and not US; these were correlated with NFP findings. Contrary to US, fetal MR imaging provides good delineation of the cerebral sulci and the ventricular walls (7, 9, 12, 13). Our results showed that a T2-weighted sequence is the best sequence for delineating the fetal brain and hence to accurately evaluate sulci development.

Cerebral Parenchyma

In 24 fetuses, MR images depicted parenchymal lesions not shown on sonograms. In nine fetuses, ventriculomegaly was the only pathologic sign revealed by US. This fact highlights the role of MR imaging in refining the etiologic diagnosis of ventricular dilatation. In cases of ventriculomegaly, the presence of associated abnormalities is a sign of a bad prognosis (14, 15); of course, this includes ischemic lesions.

In this series, the depiction of parenchymal lesions with MR imaging emphasizes the need to use different types of sequences and not merely ultrafast T2-weighted sequences. The eight hyperintense lesions revealed on T1-weighted images were markedly less well shown or even completely overlooked on T2-weighted images (Fig 1), with slight T2 hypointensity in three lesions and T2 isointense signal in five lesions.

Indeed, ultrafast T2-weighted sequences are limited by T2 decay during data collection that causes blurring of the images along the phase-encoding direction. Therefore, the signal-to-noise and signal-to-contrast ratios are decreased; this decrease is particularly pronounced for some tissues with a relatively short T2 and causes possible loss of these tissues on the images (zref16–18).

GRE T2*-weighted imaging may depict hemosiderin deposits or calcifications that create a magnetic dipole and generate interference on intravoxel parameters that is responsible for a signal intensity loss (19). Therefore, this sequence is accurate for detecting chronic hemorrhagic lesions possibly associated with ischemia. This sequence has a low signal-to-noise ratio and provides poor depiction of the cerebral anatomy and parenchyma. It must therefore be combined with T2- and T1-weighted imaging.

NFP Findings

The patterns and locations of the consequences of an insult vary during pregnancy. The fetal brain has a limited capacity for astrocytic reaction. Before 20–21 weeks' gestation, an insult results in parenchymal necrosis without gliosis; hence, a porencephalic cavity appears. After 26 weeks' gestation, the insult leads to intense astrocytic proliferation, which results in a septate cavity with irregular walls. The later the insult occurs, the more often a pure gliosis with no cystic component is observed (3, 20).

Before 34–36 weeks' gestation, white matter—particularly the periventricular white matter—is the most vulnerable zone. After this stage, this zone is displaced to the subcortical white matter and cortex because of changes in cerebral vascularization (2, 3). Moreover, the germinal zone is particularly sensitive to variations of blood pressure, hypoxia, and anoxia (3, 5, 21).

Comparison between MR imaging and NFP findings shows a good correlation between both examinations. Concerning the evaluation of parenchymal lesions, MR findings were always confirmed by NFP results. Hyperintense lesions on T1-weighted images were correlated to laminar necrosis or some forms of periventricular leukomalacia. The mechanism of this hyperintensity in laminar necrosis is uncertain and might result from the denaturation of some proteins (22). In periventricular leukomalacia, the hyperintensity is attributed to microcalcification similar to that observed in neonates (3); this was observed in the MR imaging–NFP correlations of our series.

The focal T2 hyperintensities in the cerebral parenchyma were particularly intense when they corresponded to cavitary lesions. In most cases, they were located in the white matter and sometimes in the basal ganglia. Gliosis appeared as less marked hyperintensity. The contrast between a lesion and the fetal parenchyma is reduced because of the high water content of the fetal brain and its incomplete myelination (23). Consequently, detecting a pathologic hyperintensity within the physiologic hyperintensity of the white matter can prove difficult, as observed in preterm neonates (24). This may explain the fact that, in 10 fetuses, NFP examination showed lesions that were more extensive than suggested by MR imaging. This retrospective study included many cases in which MR imaging was performed some years ago without diffusion tensor imaging; therefore, the accuracy of this technique could not be evaluated in this series. Measuring apparent diffusion coefficient at different points in the brain, as reported in neonates (25, 26), would make it possible to detect white matter abnormalities at an earlier stage and in a more objective manner. Standards have been established in two series of 15 (27) and 25 (28) fetuses.

In four other lesions, NFP yielded additional data. Two cases of polymicrogyria were overlooked at MR imaging. One fetus had a huge bilateral subdural hematoma that was responsible for compression of both hemispheres so that the surface of the brain could not be analyzed during imaging. The other fetus had diffuse clastic lesions with porencephalic cavities and marked thinning of the cerebral parenchyma that could not be properly analyzed with MR imaging.

Two diffuse periventricular ischemic lesions were overlooked during MR imaging in two fetuses with

marked or rapidly progressing ventriculomegaly. It is generally accepted in the literature that patients with severe (>15 mm) or rapidly increasing ventricular dilatations often have a bad prognosis (17, 29, 30).

Conclusion

Fetal MR imaging is a valuable tool in the evaluation of fetal brain ischemia involving either the cortex (polymicrogyria, laminar necrosis) or the white matter. To detect ischemic lesions, it is not sufficient to perform only T2-weighted sequences. T1-weighted images are mandatory in this context, because laminar necrosis and calcified leukomalacia is revealed only with this type of sequence. Moreover, T2*-weighted sequences may also be valuable in the detection of old hemorrhagic lesions. MR imaging is more accurate in detecting small focal lesions than in evaluating diffuse white matter abnormalities. In the future, diffuse tensor imaging will undoubtedly help in detecting these microstructural changes and in assessing diffuse ischemic damage.

Acknowledgment

The authors would like to thank Magali Nater for her valuable assistance in preparing the manuscript.

References

1. Garel C, Delezoide AL, Guibaud L, Sebag G, Gressens P. *Imagerie du Cerveau Fœtal Pathologique.* Sauramps Médical: Montpellier, France; 2002
2. Vannucci RC. **Hypoxic-ischemic encephalopathy**. *Am J Perinatol* 2000;17:113–120
3. Barkovich AJ. **Brain and spine injuries in infancy and childhood.** In: *Congenital malformations of the brain and skull in Pediatric Neuroimaging.* Philadelphia; Lippincott, Williams & Wilkins; 2000;157–249
4. Fusch C, Ozdoba C, Kuhn P, et al. **Perinatal ultrasonography and magnetic resonance imaging findings in congenital hydrocephalus associated with fetal intraventricular hemorrhage**. *Am J Obstet Gynecol* 1997;177:512–518
5. Rorke LB, Zimmerman RA. **Prematurity, postmaturity and destructive lesions in utero**. *AJNR Am J Neuroradiol* 1992;13:517–536
6. De Laveaucoupet J, Audibert F, Guis F, et al. **Fetal magnetic resonance imaging (MRI) of ischemic brain injury**. *Prenat Diagn* 2001;21:729–736
7. Garel C, Chantrel E, Brisse H, et al. **Fetal cerebral cortex: normal gestational landmarks identified using prenatal MR imaging**. *AJNR Am J Neuroradiol* 2001;22:184–189
8. Garel C, Chantrel E, Sebag G, Brisse H, Elmaleh M, Hassan M. *Le Développement du Cerveau Fœtal: Atlas IRM et Biométrie.* Sauramps Médical: Montpellier, France; 2000
9. Garel C, Chantrel E, Elmaleh M, Brisse H, Sebag G. **Fetal MRI: normal gestational landmarks for cerebral biometry, gyration and myelination**. *Child Nerv Syst* 2003;19:422–425
10. Barkovich AJ. **Brain and spine injuries in infancy and childhood.** In: *Congenital Malformations of the Brain and Skull in Pediatric Neuroimaging.* Philadelphia: Lippincott, Williams & Wilkins 2000;157–249
11. Rorke LB, Zimmerman RA. **Prematurity, postmaturity and destructive lesions in utero**. *AJNR Am J Neuroradiol* 1992;13:517–536
12. Levine D. Barnes PD. **Cortical maturation in normal and abnormal fetuses as assessed with prenatal MR imaging**. *Radiology* 1999;210:751–758
13. Adamsbaum C, Gelot A, André C, Baron JM. *Atlas d'IRM du Cerveau Fœtal.* Masson: Paris, France; 2001
14. Bannister CM, Russel SA, Rimmer S, Arora A. **Pre-natal ventriculomegaly and hydrocephalus**. *Neurol Res* 2000;22:37–42.
15. Durfee SM, Kim FM, Benson CB. **Postnatal outcome of fetuses with the prenatal diagnosis of asymmetric hydrocephalus**. *J Ultrasound Med* 2001;20:263–268
16. Huisman T A. G. M., Martin E. Kubik-Huch R, Marincek B. **Fetal magnetic resonance imaging of the brain: technical considerations and normal brain development**. *Eur Radiol* 2002;12:1941–1951
17. Ertl-Wagner B, Lienemann A, Strauss A, Reiser MF. **Fetal magnetic resonance imaging: indications, technique, anatomical considerations and a review of fetal abnormalities**. *Eur Radiol* 2002;12:1931–1940
18. Penzkofer AK, Pfluger T, Pochmann Y, Meissner O, Leinsinger G. **MR Imaging of the brain in pediatric patients: diagnostic value of Haste sequences**. *AJR Am J Roentgenol* 2002;179:509–514
19. Duchêne M, Caldas JGMP, Benoudiba F, Cerri GG, Doyon D. **Comparative study of MR sequences to detect cavernous angiomas.** *J Radiol* 2002;83:1843–1846
20. Simon EM, Goldstein RB, Coakley FV, et al. **Fast MR imaging of fetal CNS anomalies in utero**. *AJNR Am J Neuroradiol* 2000;21:1688–1698
21. Fukui K, Morioka T, Nishio S, et al. **Fetal germinal matrix and intraventricular haemorrhage diagnosed by MRI**. *Neuroradiology* 2001;43:68–72
22. Brisse H, Fallet C, Sebag G, Nessmann C, Blot P, Hassan M. **Supratentorial parenchyma in the developing fetal brain: in vitro MR study with histologic comparison**. *AJNR Am J Neuroradiol* 1997;18:1491–1497
23. Counsell SJ, Maalouf EF, Fletcher AM, et al. **MR Imaging assessment of myelination in the very preterm brain**. *AJNR Am J Neuroradiol* 2002;23:872–881
24. Panigrahy A, Barnes PD, Robertson RL, et al. **Volumetric brain differences in children with periventricular T2-signal hyperintensities: a grouping by gestational age at birth**. *AJR Am J Roentgenol* 2001;177:695–702
25. Neil JJ, Shiran SI, McKinstry RC, et al. **Normal brain in human newborns: apparent diffusion coefficient and diffusion anisotropy measured by using diffusion tensor MR imaging**. *Radiology* 1998;209:57–66
26. Hüppi PS, Maier SE, Peled S, et al. **Microstructural development of human newborn cerebral white matter assessed in vivo by diffusion tensor magnetic resonance imaging**. *Pediatr Res* 1998;44:584–590
27. Righini A, Bianchini E, Parazzini C, et al. **Apparent diffusion coefficient determination in normal fetal brain: a prenatal MR imaging study**. *AJNR Am J Neuroradiol* 2003;24:799–804
28. Bui T, Daire Jl, Alberti C, et al. **Microstructural development of fetal brain assessed in utero by diffusion tensor imaging**. *Pediatr Radiol* 2003;33:S26
29. Wilhelm C, Keck C, Hess S, Korinthenberg, Breckwoldt M. **Ventriculomegaly diagnosed by prenatal ultrasound and mental development of the children.** *Fetal Diagn Ther* 1998;13:162–166
30. Arora A, Bannister CM, Russell S, Rimmer S. **Outcome and clinical course of prenatally diagnosed cerebral ventriculomegaly [Suppl]**. *Eur J Pediatr Surg* 1998;8:63–64